

# UC Irvine

## UC Irvine Previously Published Works

### Title

Protein kinase C downregulates I(Ks) by stimulating KCNQ1-KCNE1 potassium channel endocytosis.

### Permalink

<https://escholarship.org/uc/item/3b61q6v1>

### Journal

Heart rhythm, 8(10)

### ISSN

1547-5271

### Authors

Kanda, Vikram A  
Purtell, Kerry  
Abbott, Geoffrey W

### Publication Date

2011-10-01

### DOI

10.1016/j.hrthm.2011.04.034

### Copyright Information

This work is made available under the terms of a Creative Commons Attribution License, available at <https://creativecommons.org/licenses/by/4.0/>

Peer reviewed

# Protein kinase C downregulates $I_{Ks}$ by stimulating KCNQ1-KCNE1 potassium channel endocytosis

Vikram A. Kanda, PhD, Kerry Purtell, BA, Geoffrey W. Abbott, MSc, PhD

From the Department of Pharmacology, Weill Medical College of Cornell University, New York, New York.

**BACKGROUND** The slow-activating cardiac repolarization  $K^+$  current ( $I_{Ks}$ ), generated by the KCNQ1-KCNE1 potassium channel complex, is controlled via sympathetic and parasympathetic regulation in vivo. Inherited KCNQ1 and KCNE1 mutations predispose to ventricular fibrillation and sudden death, often triggered by exercise or emotional stress. Protein kinase C (PKC), which is activated by  $\alpha_1$  adrenergic receptor stimulation, is known to downregulate  $I_{Ks}$  via phosphorylation of KCNE1 serine 102, but the underlying mechanism has remained enigmatic. We previously showed that KCNE1 mediates dynamin-dependent endocytosis of KCNQ1-KCNE1 complexes.

**OBJECTIVE** This study sought to determine the potential role of endocytosis in  $I_{Ks}$  downregulation by PKC.

**METHODS** We utilized patch clamping and fluorescence microscopy to study Chinese hamster ovary (CHO) cells coexpressing KCNQ1, KCNE1, and wild-type or dominant-negative mutant (K44A) dynamin 2, and neonatal mouse ventricular myocytes.

**RESULTS** The PKC activator phorbol 12-myristate 13-acetate (PMA) decreased  $I_{Ks}$  density by >60% ( $P < .05$ ) when coexpressed with wild-type dynamin 2 in CHO cells, but had no effect when

coexpressed with K44A-dynamin 2. Thus, functional dynamin was required for downregulation of  $I_{Ks}$  by PKC activation. PMA increased KCNQ1-KCNE1 endocytosis in CHO cells expressing wild-type dynamin 2, but had no effect on KCNQ1-KCNE1 endocytosis in CHO cells expressing K44A-dynamin 2, determined using the Pearson correlation coefficient to quantify endosomal colocalization of KCNQ1 and KCNE1 with internalized fluorescent transferrin. KCNE1-S102A abolished the effect of PMA on  $I_{Ks}$  currents and endocytosis. Importantly, PMA similarly stimulated endocytosis of endogenous KCNQ1 and KCNE1 in neonatal mouse myocytes.

**CONCLUSION** PKC activation downregulates  $I_{Ks}$  by stimulating KCNQ1-KCNE1 channel endocytosis.

**KEYWORDS** Endocytosis;  $I_{Ks}$ ; KCNE1; KCNQ1; PKC; Trafficking

**ABBREVIATIONS** CHO = Chinese hamster ovary;  $I_{Ks}$  = slow-activating cardiac delayed rectifier  $K^+$  current; LQT = long QT; PBS = phosphate-buffered saline; PKC = protein kinase C; PMA = phorbol 12-myristate 13-acetate.

(Heart Rhythm 2011;8:1641-1647) © 2011 Heart Rhythm Society. All rights reserved.

## Introduction

Voltage-gated potassium channels open in response to cellular depolarization and repolarize the cell membrane by facilitating  $K^+$  efflux, thus regulating electrical excitability and the action potential repolarization profile of excitable cells. Voltage-gated potassium channels exhibit significant diversity, differing in their conductance, voltage dependence, gating kinetics, and pharmacology.<sup>1</sup> This functional diversity is facilitated in part by posttranslational modifications and association of the pore-forming ( $\alpha$ ) subunits with ancillary ( $\beta$ ) subunits, including the single transmembrane segment KCNE subunits (also known as MinK-related peptides).<sup>2</sup>

KCNE1 (also known as MinK) co-assembles with the KCNQ1 (Kv7.1)  $\alpha$  subunit to generate  $I_{Ks}$ , the slowly activating human cardiac ventricular repolarization  $K^+$  current.<sup>3-6</sup>  $I_{Ks}$

is also present in the inner ear, where it helps maintain fluid homeostasis.<sup>7,8</sup> KCNE1 slows KCNQ1 activation 5- to 10-fold, increases its unitary conductance 4-fold, and eliminates inactivation.<sup>5,9,10</sup> KCNQ1 and KCNE1 loss-of-function mutations are associated with long QT (LQT) syndrome, in which delayed ventricular myocyte repolarization causes arrhythmogenic events including early afterdepolarizations, predisposing to ventricular arrhythmias. Patients with KCNQ1 (LQT1) or KCNE1 (LQT5) mutations are classified as having either Romano-Ward syndrome, which is generally autosomal dominant, or the Jervell and Lange-Nielsen cardioauditory syndrome, which typically requires mutations in both alleles.<sup>11-13</sup>

KCNQ1-KCNE1 is highly regulated by the autonomic nervous system in vivo. In individuals with loss-of-function KCNQ1 mutations, cardiac events, including ventricular fibrillation and sudden cardiac death, often occur during exercise or in times of emotional stress, when there is an abrupt sympathetic activation. Staggeringly, KCNQ1 mutations have accounted for two-thirds of cases of drowning or near drowning in which the individual's DNA was sequenced because of a suspected channelopathic link. Swimming is suggested to be a particularly high-risk activity

Supported by grants HL079275 and HL101190 from the National Institutes of Health/National Heart, Lung, and Blood Institute to G.W.A., who is the recipient of an Irma T. Hirschl Career Scientist Award. **Address reprint requests and correspondence:** Dr. Geoffrey W. Abbott, Department of Pharmacology, Box 70, Weill Cornell Medical College, New York, NY 10021. E-mail address: gwa2001@med.cornell.edu. (Received March 23, 2011; accepted April 29, 2011.)

because it increases both sympathetic and parasympathetic activation, incorporating exercise, voluntary apnea, and the dive reflex activated by facial immersion.<sup>14,15</sup>

The voltage-gated potassium channel subunit composition and half-life at the plasma membrane dictate their contribution to repolarization and excitability. We previously discovered that 3 sites on the intracellular C-terminus of KCNE1 are required for clathrin- and dynamin-dependent endocytosis of the KCNQ1-KCNE1 channel complex, redefining KCNE1 as an endocytic chaperone for KCNQ1.<sup>16</sup> One of these sites, KCNE1-S102, is phosphorylated by protein kinase C (PKC), resulting in decreased  $I_{Ks}$  current density in human, rat, and mouse. In contrast, guinea pig  $I_{Ks}$  is not downregulated by PKC because guinea pig KCNE1 has an asparagine, not a serine, at position 102.<sup>17-19</sup> Although this mode of  $I_{Ks}$  regulation was described 2 decades ago, the underlying mechanism for KCNE1-S102 phosphorylation leading to  $I_{Ks}$  downregulation has not previously been reported. PKC downregulation of  $I_{Ks}$  is potentially of pathophysiological importance, because  $\alpha 1$  adrenergic agonists, including norepinephrine, activate PKC in cardiac myocytes,<sup>20</sup> and are also known to prolong the plateau phase in cardiac myocytes, with a variety of suggested contributory mechanisms.<sup>21</sup> Here, we show that the inhibitory effect of PKC on  $I_{Ks}$  can be explained by increased internalization of KCNQ1-KCNE1 from the plasma membrane.

## Methods

### Cell culture and transfection

CHO cells were cultured and transfected as previously described,<sup>16,22</sup> using SuperFect transfection reagent (Qiagen, Hilden, Germany) with cDNA as follows: 2  $\mu$ g human KCNQ1 cDNA and 1  $\mu$ g human KCNE1 cDNA, alone or with 1  $\mu$ g wild-type or K44A dynamin 2. For electrophysiology, cells were co-transfected with cDNA encoding enhanced green fluorescent protein to facilitate detection.

Neonatal mouse ventricular myocytes were isolated and cultured as follows: ventricles from P1 C57BL/6 neonatal mice were excised and washed in Hank's balanced salt solution (American Type Culture Collection [ATCC]). Tissue was digested in collagenase type II (Worthington Biochemicals, Lakewood, NJ) and passed through a cell strainer (BD Biosciences, San Jose, CA). Cells were pelleted and resuspended in Dulbecco's Modified Eagle's Medium (ATCC), supplemented with Fetal Bovine Serum (FBS), and incubated at 37°C gassed with 5% CO<sub>2</sub>.

### Electrophysiology

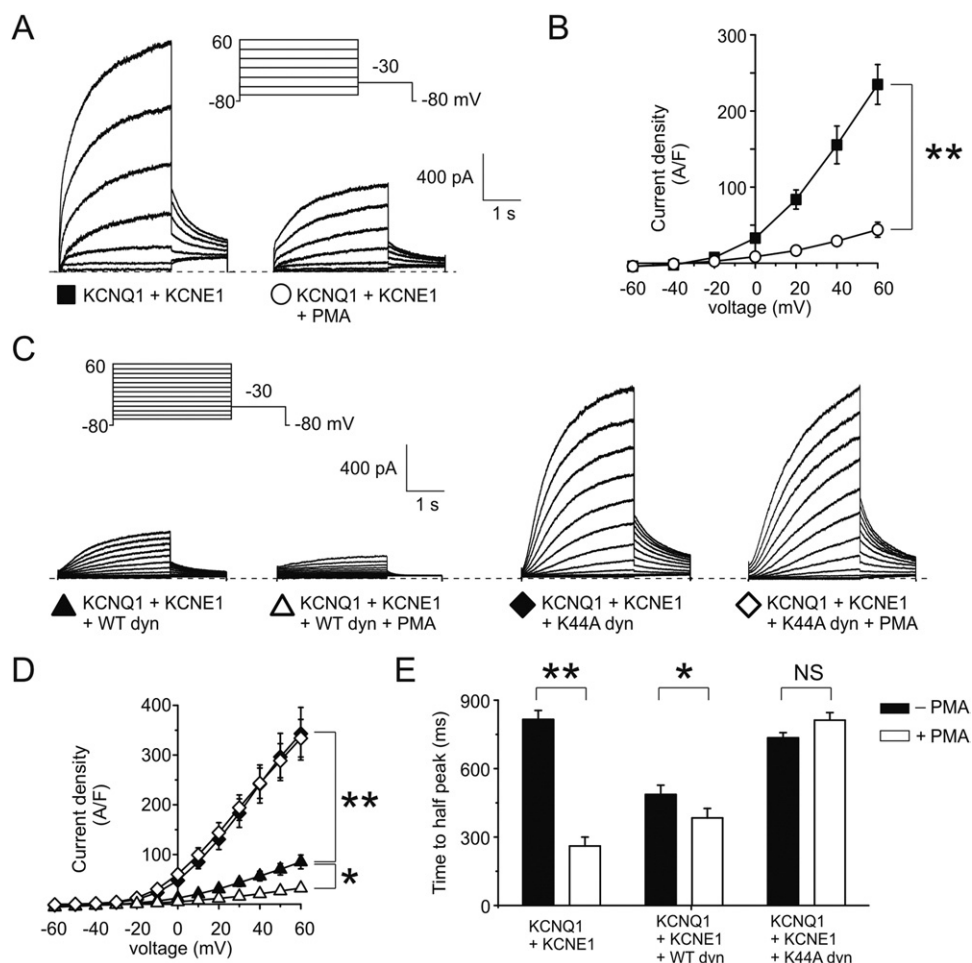
Electrophysiological recordings from transiently transfected CHO cells were performed by voltage clamp using the whole-cell configuration of the patch-clamp technique as previously described.<sup>22</sup> Briefly, whole-cell currents were recorded at room temperature using a Multiclamp 700A amplifier (Axon Instruments, Foster City, CA), and data acquisition and analysis were performed using the pCLAMP 9.0 software suite (Axon Instruments). Cells were perfused with an extracellular bath solution containing (in mM) 135 NaCl, 5 KCl, 1.2 MgCl<sub>2</sub>, 5 HEPES, 2.5 CaCl<sub>2</sub>, 10 D-glucose (pH 7.4). Patch electrodes

were pulled from standard-walled, borosilicate glass capillaries with filament (Sutter Instruments, Novato, CA) using a P-97 horizontal puller (Sutter Instruments) and had resistances of 3 to 5 M $\Omega$  when filled with intracellular solution containing (in mM): 10 NaCl, 117 KCl, 2 MgCl<sub>2</sub>, 11 HEPES, 11 EGTA, 1 CaCl<sub>2</sub> (pH 7.2). Data were filtered at 1 kHz and digitized at 5 kHz using a Digidata 1322A analogue-to-digital converter (Axon Instruments). For analysis of voltage dependence and activation kinetics, cells were held at -80 mV and subjected to 3-second test pulses from -60 mV to +60 mV in either 10- or 20-mV increments, followed by a 2-second tail pulse to -30 mV. For experiments with phorbol 12-myristate 13-acetate (PMA) (Sigma-Aldrich, St. Louis, MO), cells were incubated with PMA (50 nM) in F12K medium for 30 minutes at 37°C immediately prior to patching. Data were analyzed using Clampfit 9.0 software (Axon Instruments), and graphs were generated using Origin 6.0 (Microcal Commerce, CA). Data are expressed as mean  $\pm$  SEM of observations from  $n$  cells. Statistical significance was assessed by 1-way analysis of variance, with  $P < .05$  being indicative of significance.

### Fluorescence microscopy

For fluorescence microscopy, CHO cells were transfected as described previously, but green fluorescent protein-tagged human KCNQ1 and hemagglutinin-tagged human KCNE1 were used to facilitate detection 48 hours after transfection, as before.<sup>16,22</sup> After transfection, the cells were lysed, trypsinized, and moved from 60-mm dishes to Culturewell chambered coverglass (Invitrogen, Carlsbad, CA). To label endosomes containing proteins internalized over a 30-minute period, both CHO cells and neonatal mouse ventricular myocytes were washed once in phosphate-buffered saline (PBS) and incubated with Alexa Fluor 594-conjugated transferrin (Invitrogen) in F12K medium for 30 minutes at 37°C. For PMA treatment, cells were incubated with PMA in F12K medium for 30 minutes at 37°C. After this, cells were washed once again and fixed in ice-cold 4% Paraformaldehyde (PFA) in PBS for 30 minutes at room temperature. Cells were then washed twice with ice-cold PBS for 1 minute each wash. The cells were subsequently permeabilized using 0.25% Triton-X-100 in PBS for 10 minutes at room temperature and then washed 3  $\times$  5 minutes in PBS. After blocking for 30 minutes in 1% Bovine Serum Albumin (BSA)/PBS, cells were incubated with primary antibodies for 1 hour at room temperature. For CHO cells, mouse monoclonal antihemagglutinin 7 (1:1,000, Sigma) was utilized to detect hemagglutinin-tagged KCNE1. For myocytes, goat polyclonal anti-KCNQ1 (1:50, Santa Cruz Biotechnology, Santa Cruz, CA) and rabbit polyclonal anti-KCNE1 (1:100; Alamone, Jerusalem, Israel) were utilized to detect the endogenous subunits. The cells were next rinsed and incubated with secondary antibodies (1:1000) [Alexa Fluor 488 donkey anti-rabbit immunoglobulin G (H+L) or Alexa Fluor 350 donkey antimouse (or antigoat) immunoglobulin G (H+L) (Invitrogen)] in 1% BSA/PBS in the dark for 1 hour at room temperature. The cells were washed again for 3  $\times$  5 minutes in PBS before mounting on slides in Prolong antifade mounting medium. Slides were allowed to set overnight before viewing on

**Figure 1** PKC downregulation of  $I_{Ks}$  requires functional dynamin. **A:** Exemplar traces showing currents recorded in CHO cells co-transfected with cDNA encoding KCNQ1 and KCNE1, untreated or after treatment with PMA (50 nM, 30 minutes), as indicated. Voltage protocol inset. **B:** Mean peak current density from CHO cells transfected with cDNA encoding KCNQ1 and KCNE1 untreated ( $n = 73$ ) or after treatment with PMA ( $n = 25$ ); symbols as in A.  $**P < .001$ . **C:** Exemplar traces showing currents recorded in CHO cells co-transfected with cDNA encoding KCNQ1, KCNE1, and either wild-type dynamin 2 or K44A dynamin 2, untreated or after treatment with PMA (50 nM), as indicated. Voltage protocol inset. **D:** Mean peak current density from CHO cells co-transfected with cDNA encoding KCNQ1, KCNE1, and wild-type dynamin 2, untreated ( $n = 18$ ) or after treatment with PMA ( $n = 6$ ); or KCNQ1, KCNE1, and K44A dynamin 2, untreated ( $n = 20$ ) or after treatment with PMA ( $n = 6$ ); symbols as in C.  $*P < .05$ ;  $**P < .001$ . **E:** Time-to-half-peak current at +60 mV for cells co-expressing KCNQ1 and KCNE1, alone or with either wild-type or K44A dynamin 2, with or without PMA treatment, as indicated;  $n$  values as in D.  $*P < .05$ ;  $**P < .001$ .  $I_{Ks}$  = slow-activating cardiac delayed rectifier  $K^+$  current; CHO = Chinese hamster ovary; PKC = protein kinase C; PMA = phorbol 12-myristate 13-acetate.



an Olympus BX51 fluorescence microscope (Olympus, Tokyo, Japan). Pictures were acquired using cellSens Standard digital imaging software (Olympus). Colocalization of KCNQ1, KCNE1, and transferrin was quantified using the Pearson correlation coefficient, determined through intensity correlation analysis<sup>23</sup> with ImageJ software (NIH, Bethesda, MD), using the MBF ImageJ for Microscopy collection of plug-ins (McMaster Biophotonics Facility, Hamilton, ON, Canada).

## Results

### PKC downregulates $I_{Ks}$ via a dynamin-dependent mechanism

CHO cells transfected with KCNQ1 and KCNE1 cDNA exhibited slowly activating, noninactivating currents, measured using whole-cell voltage clamp (Figures 1A and 1B). Activation of PKC by phorbol esters was previously reported to reduce  $I_{Ks}$  by phosphorylation of serine 102 on KCNE1.<sup>17–19</sup> Consistent with these previous reports, activation of PKC by the phorbol ester PMA downregulated  $I_{Ks}$  by >70% ( $P < .001$ ) (Figures 1A and 1B).

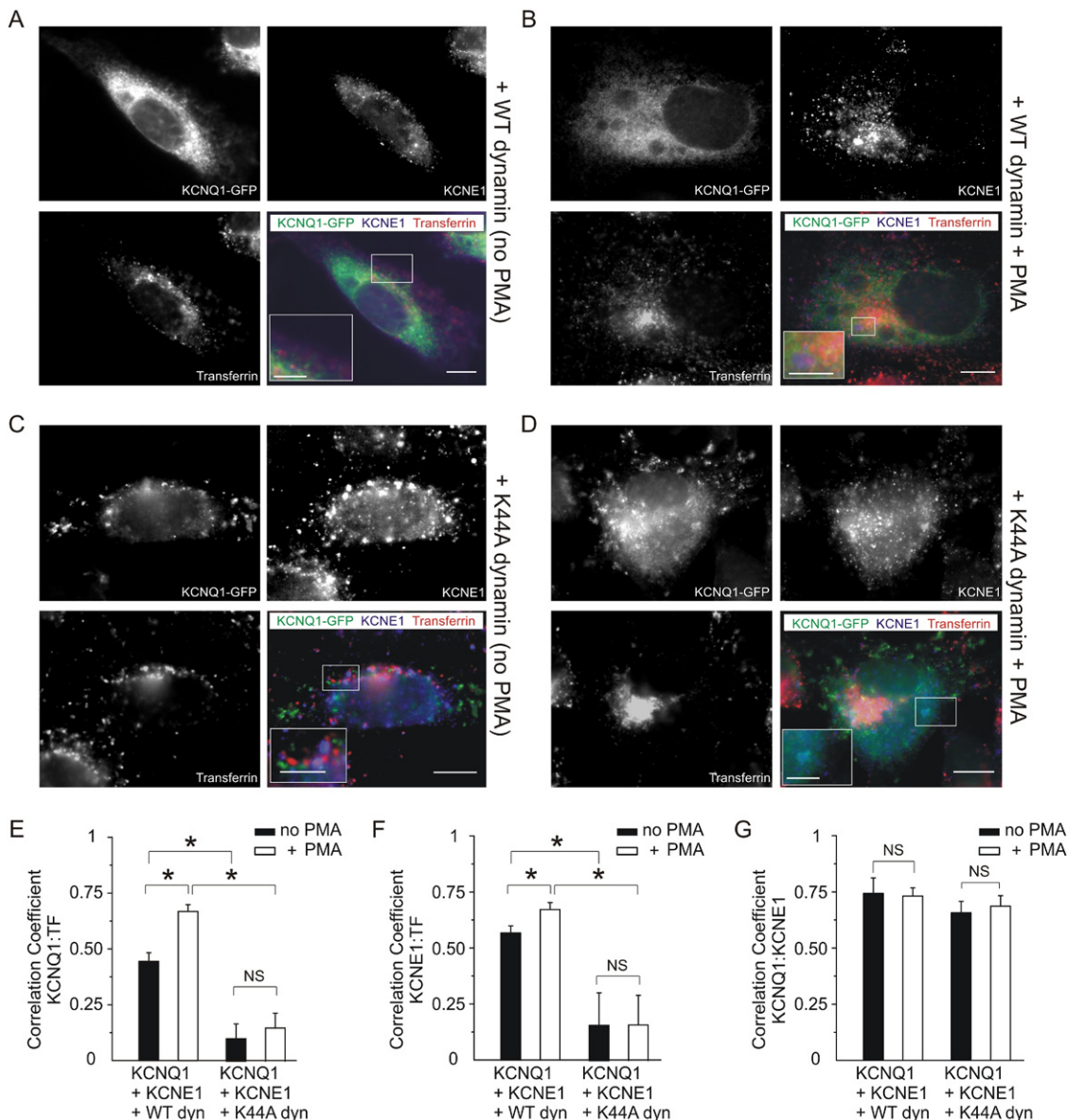
Dynamin is a guanosine triphosphatase that is required for the pinching off of clathrin-coated pits during endocytosis; dynamin 2 is the isoform that is ubiquitously expressed but enriched in heart and skeletal muscle, whereas dynamin 1 and

3 are neuronal- and testis-specific, respectively.<sup>24</sup> Herein, to assess the potential role of dynamin-dependent endocytosis in PKC-induced  $I_{Ks}$  downregulation, we utilized both the wild-type form of dynamin 2 (as a positive control) and the dominant-negative mutant K44A dynamin 2, which inhibits clathrin-mediated endocytosis and other forms of dynamin-dependent endocytosis.<sup>25</sup> We first observed that K44A dynamin 2 increased  $I_{Ks}$  4-fold compared to cells co-transfected with wild-type dynamin 2 ( $P < .001$ ) (Figures 1C and 1D), consistent with our previous findings.<sup>16</sup> We also found that mean  $I_{Ks}$  density in cells without overexpressed, exogenous dynamin 2 (Figures 1A and 1B) was intermediate between that of cells expressing exogenous wild-type dynamin 2 and those expressing exogenous K44A dynamin 2 (Figures 1C and 1D). This indicated, as expected from our previous study,<sup>16</sup> that there was some endogenous dynamin activity in CHO cells. Strikingly, we next found that PMA treatment did not alter  $I_{Ks}$  density when KCNQ1 and KCNE1 were coexpressed with K44A dynamin 2, but downregulated  $I_{Ks}$  >60% ( $P < .05$ ) when KCNQ1 and KCNE1 were coexpressed with wild-type dynamin 2 (Figures 1C and 1D). Thus, functional dynamin was required for the inhibitory effect of PKC on  $I_{Ks}$ .

Previously, we found that increasing dynamin-dependent endocytosis of KCNQ1-KCNE1 complexes increased the

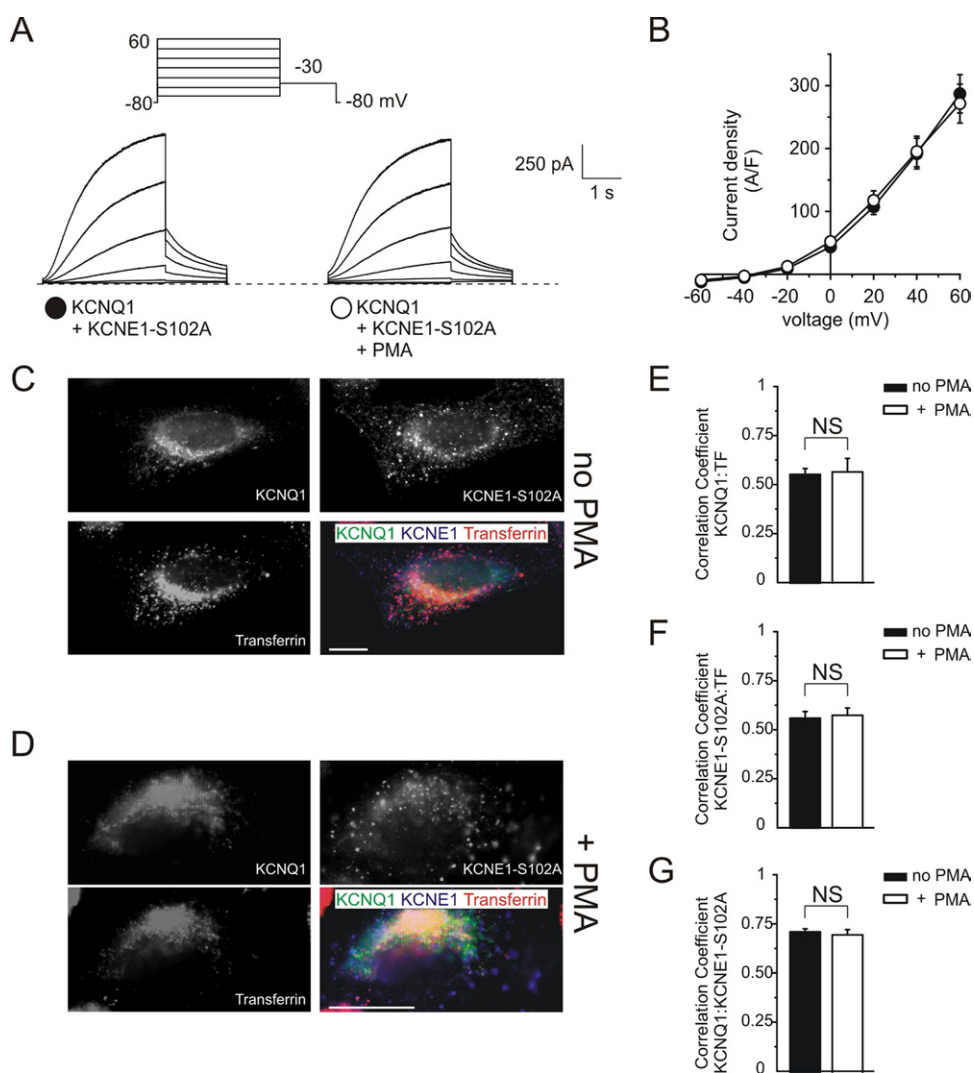
activation rate of currents in cells co-transfected with KCNQ1 and KCNE1.<sup>16</sup> This occurs because only complexes containing KCNE1 are internalized by a dynamin-dependent mechanism, therefore decreasing the relative amount of surface-expressed KCNQ1-KCNE1 compared to homomeric KCNQ1,<sup>16</sup> which activates more rapidly without KCNE1 (but has a lower unitary conductance). Here, we discovered that the activation rate of currents expressed in CHO cells transfected with KCNQ1 and KCNE1 alone or

with wild-type dynamin 2 was also significantly increased by PMA, but that co-transfection of K44A dynamin 2 removed the capacity of PMA to alter activation rate (Figure 1E). Indeed, current activation in PMA-treated cells coexpressing KCNQ1, KCNE1, and K44A dynamin 2 was not significantly different from cells expressing only KCNQ1 and KCNE1, in the absence of PMA. The data in Figure 1 indicate that functional dynamin is required for PKC to down-regulate the density but increase the activation rate of  $I_{Ks}$ .



shows paucity of cell surface KCNQ1 and KCNE1. **B:** Single-wavelength and merged images of an exemplar PMA-treated cell expressing KCNQ1, KCNE1, and wild-type dynamin 2, showing a predominantly intracellular location of KCNQ1, KCNE1, and transferrin, with regions of marked KCNQ1/transferrin and KCNE1/transferrin colocalization (mauve and orange, respectively, on merged image, see inset). **C:** Single-wavelength and merged images of an exemplar non-PMA-treated cell expressing KCNQ1, KCNE1, and K44A dynamin 2, showing marked punctate, cell-surface accumulation of KCNQ1 and KCNE1, often not co-localizing with transferrin (inset on merged image). **D:** Single-wavelength and merged images of an exemplar PMA-treated cell expressing KCNQ1, KCNE1, and K44A dynamin 2, showing a marked nonpunctate, intracellular concentration of transferrin (consistent with PKC-stimulated macropinocytosis<sup>34</sup>) versus broad intracellular and surface punctate distribution of KCNQ1 and KCNE1. Inset on merged image shows KCNQ1-KCNE1 colocalization (aquamarine). **E-G:** Quantification of colocalization of images as in A to D with wild-type or K44A dynamin 2, with or without PMA, as indicated, using the Pearson correlation coefficient,  $n = 5$  cells per group. \* $P < .05$ . **E:** KCNQ1 and transferrin; **F:** KCNE1 and transferrin; **G:** KCNQ1 and KCNE1. Abbreviations as in Figure 1.

**Figure 3** KCNE1-S102A controls PKC-dependent KCNQ1-KCNE1 endocytosis. **A:** Exemplar traces showing currents recorded in CHO cells co-transfected with cDNA encoding KCNQ1 and KCNE1-S102A, untreated or after treatment with PMA (50 nM, 30 minutes), as indicated. Voltage protocol inset. **B:** Mean peak current density from CHO cells transfected with cDNA encoding KCNQ1 and KCNE1-S102A untreated ( $n = 10$ ) or after treatment with PMA ( $n = 10$ ); symbols as in A. **C, D:** Fluorescence microscopy of CHO cells co-transfected with KCNQ1-green fluorescent protein (green) and human KCNE1-S102A (blue), as indicated. Live cells were incubated with fluorescent transferrin (red) and with PMA (50 nM for 30 minutes) to activate PKC where indicated. Single-wavelength fluorescence images are shown in monochrome for clarity, with the corresponding merged (triple-wavelength) images shown in color. Scale bars: 5  $\mu\text{m}$ . **C:** Exemplar non-PMA-treated cell expressing KCNQ1 and KCNE1-S102A. **D:** Exemplar PMA-treated cell expressing KCNQ1 and KCNE1-S102A. **E–G:** Quantification of colocalization of images as in C and D with and without PMA, as indicated, using the Pearson correlation coefficient,  $n = 5$  cells per group. **E:** KCNQ1 and transferrin; **F:** KCNE1-S102A and transferrin; **G:** KCNQ1 and KCNE1-S102A. Abbreviations as in Figure 1.



### PKC activation increases clathrin-mediated, dynamin-dependent endocytosis of KCNQ1-KCNE1 complexes

We next used fluorescence microscopy to examine whether PMA induces clathrin- and dynamin-dependent endocytosis of KCNQ1-KCNE1, utilizing co-transfected dynamin 2, and fluorescently labeled transferrin fed to live cells—an established marker of endosomes involved in clathrin-mediated endocytosis<sup>26</sup> (Figure 2). KCNQ1 and KCNE1 subunits strongly colocalized with one another (Pearson correlation coefficient =  $0.75 \pm 0.06$ ,  $n = 5$ ) and were predominantly located intracellularly, with little cell surface accumulation, when expressed with wild-type dynamin 2 (Figures 2A and 2G). Treatment of these cells with PMA resulted in a similar pattern (Figure 2B) but significantly increased the colocalization of KCNQ1 and KCNE1 with internalized transferrin (Figures 2E and 2F;  $P < .05$ ,  $n = 5$ ), without altering KCNQ1 colocalization with KCNE1 (Figure 2G).

In contrast, coexpression of KCNQ1 and KCNE1 with K44A dynamin 2 resulted in marked cell-surface accumulation of KCNQ1 and KCNE1, in a punctate pattern, regardless of PMA treatment (Figures 2C and 2D). Accordingly, coexpres-

sion with K44A dynamin 2 resulted in a comparatively low occurrence of KCNQ1 and KCNE1 in transferrin-labeled endosomes (Pearson correlation coefficient of  $<0.2$  in each case;  $n = 5$ ), and PMA did not significantly alter this (Figures 2E and 2F;  $P > .05$ ;  $n = 5$ ). Colocalization of KCNQ1 and KCNE1 with one another was not significantly affected by the type of co-transfected dynamin or by PMA treatment (Figure 2G). The data in Figure 2 indicate that in CHO cells, PKC activation by PMA decreases KCNQ1-KCNE1 channel currents by increasing clathrin- and dynamin-dependent endocytosis of KCNQ1-KCNE1 complexes.

### S102A-KCNE1 abolishes PKC-dependent KCNQ1-KCNE1 endocytosis

PKC was previously shown to downregulate  $I_{K_S}$  via phosphorylation of serine 102 in KCNE1.<sup>17–19</sup> To determine whether KCNE1 serine 102 is important for PMA-stimulated endocytosis of KCNQ1-KCNE1 complexes, we mutated serine 102 to an alanine. Consistent with previous reports, PKC activation by PMA had no effect on KCNQ1/KCNE1-S102A currents (Figures 3A and 3B). Furthermore, fluorescence microscopy confirmed that PKC activation by PMA did not affect KCNQ1/

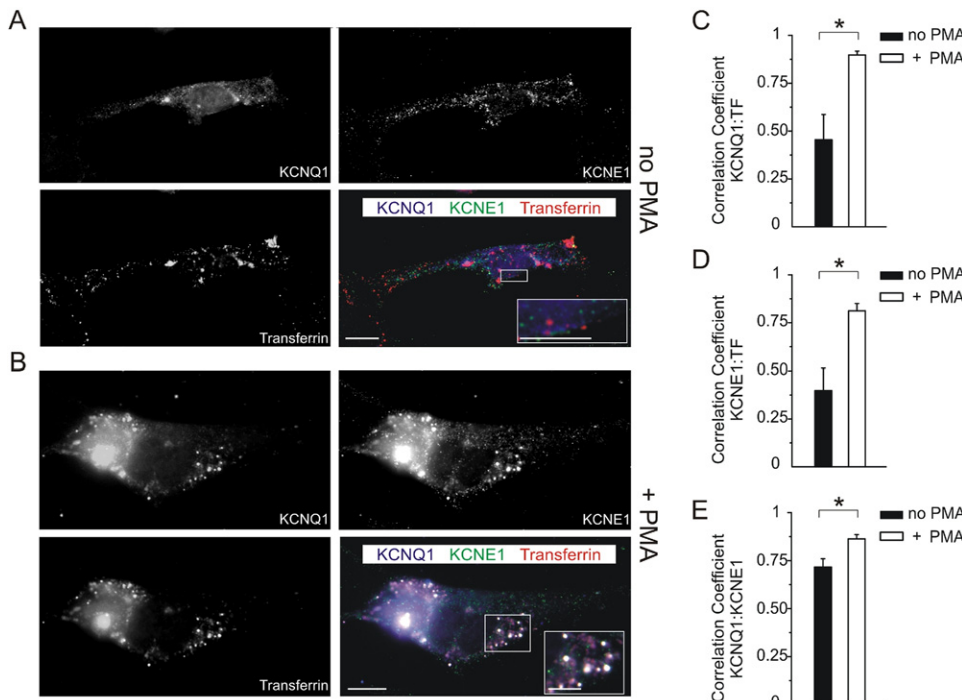


**Figure 4** PKC activation increases internalization of endogenous KCNQ1 and KCNE1 in neonatal mouse myocytes. **A, B:** Single-wavelength and merged images of exemplar neonatal mouse ventricular myocytes that were previously live-incubated with fluorescent transferrin (red) to label endosomes being actively internalized by clathrin- and dynamin-dependent endocytosis, without (**A**) or with (**B**) PMA treatment (50 nM for 30 minutes) to activate PKC. Cells were fixed and immunolabeled for KCNQ1 (blue) and KCNE1 (green). Single-wavelength fluorescence images are shown in monochrome for clarity, with the merged (triple-wavelength) images shown in color. Scale bars: 5  $\mu$ m, and 2.5  $\mu$ m for insets. **A:** Without PMA treatment, KCNQ1 and KCNE1 colocalized sometimes with one another but less so with transferrin; all 3 had a largely punctate distribution throughout the cell and at the cell surface (see inset). **B:** After PMA treatment, KCNQ1 and KCNE1 were strongly colocalized with one another and transferrin, intracellularly in endosomes (punctate pattern; white signal in merged

image indicates triple colocalization, see inset). **C–E:** Quantification of colocalization from images as in **A** and **B** with/without PMA as indicated, using the Pearson correlation coefficient,  $n = 5$  cells per group,  $*P < .05$ . **C:** KCNQ1 and transferrin; **D:** KCNE1 and transferrin; **E:** KCNQ1 and KCNE1. Abbreviations as in **Figure 1**.

KCNE1-S102A endocytosis, with no difference in the Pearson correlation coefficient for KCNE1-S102A and transferrin colocalization between untreated and PMA-treated cells (**Figures 3C to 3G**). This was consistent with our previous finding that KCNE serine 102 is influential in KCNE1-mediated, dynamin-dependent endocytosis of KCNQ1.<sup>16</sup>

### PKC activation induces the internalization of endogenous KCNQ1-KCNE1 channels in neonatal mouse ventricular myocytes

Although not highly expressed in adult mouse ventricular myocytes,  $I_{Ks}$  and its molecular correlates (KCNQ1 and KCNE1) have been previously identified in neonatal mouse ventricular myocytes.<sup>27,28</sup> To determine whether PKC activation decreases endogenous  $I_{Ks}$  by endocytosis of native KCNQ1 and KCNE1 we performed immunofluorescence studies on neonatal mouse myocytes. The results were largely consistent with those we observed in CHO cells. PMA treatment of myocytes resulted in a significant increase in intracellular colocalization of both KCNQ1 and KCNE1 with transferrin-labeled endosomes, doubling the Pearson correlation coefficient (**Figures 4B, 4C, and 4D**), compared with nontreated myocytes (**Figures 4A, 4C, and 4D**) ( $P < .05$  for PMA-treated versus nontreated cells for either subunit;  $n = 5$ ). Treatment with PMA also significantly increased colocalization of KCNQ1 with KCNE1 (**Figures 4B and 4E**), which together with the dramatic effect on internalization led to more triple co-localization between KCNQ1, KCNE1, and transferrin (white on triple-merged images, **Figure 4B**) than we had observed in CHO cells (**Figure 2**). Thus, PMA activation of

PKC results in clathrin-dependent endocytosis of endogenous KCNQ1 and KCNE1 in neonatal mouse ventricular myocytes.

### Discussion

$I_{Ks}$  provides a crucial repolarization reserve in human ventricular myocytes, being especially important in the compensatory response to action potential prolongation, thus counteracting the arrhythmogenic action of, for example,  $I_{Kr}$  antagonists. Sympathetic control of cardiac  $I_{Ks}$  density has long been known to play a role both in maintenance of normal cardiac rhythm, and in arrhythmogenesis—the classic example being incidences of sudden cardiac death while swimming in individuals with previously occult KCNQ1 mutations.<sup>14,15</sup>

Twenty years ago, several groups found that PKC activation downregulates  $I_{Ks}$  via phosphorylation of KCNE1-S102, but the underlying mechanism had remained enigmatic.<sup>17–19</sup> More recently, we found that the degree of KCNQ1-KCNE1 internalization by clathrin- and dynamin-dependent endocytosis was influenced by the residue at position 102 in KCNE1: with an aspartic acid, mimicking phosphorylated serine, KCNQ1-KCNE1 endocytosis was more extensive than if serine 102 was replaced with alanine, mimicking nonphosphorylated serine.<sup>16</sup> These data suggested clathrin- and dynamin-dependent endocytosis as a possible mechanism for PMA-induced  $I_{Ks}$  downregulation, an hypothesis confirmed by our present findings.

PKC phosphorylation of the human  $H^+K^+$ adenosine triphosphatase, ATP1A1, also causes it to be internalized by clathrin-mediated endocytosis<sup>29</sup>, setting a precedent for our findings with KCNQ1-KCNE1. KCNQ1 (independent of KCNE1) also undergoes serum- and glucocorticoid-inducible

kinase 1-dependent forward trafficking via Rab11, and internalization via Rab5.<sup>30</sup> Furthermore, KCNQ1/KCNE1 complexes can be internalized by Nedd4.2-dependent ubiquitinylation, through direct interaction of Nedd4.2 with KCNQ1<sup>31</sup>; this process was recently found to be regulated by the AMP-activated protein kinase.<sup>32</sup> Finally, short-term regulation of  $I_{Ks}$  has also been shown to occur through  $\beta$ -adrenergic receptor modulation via protein kinase A.<sup>33</sup> Thus, KCNQ1-KCNE1 trafficking is highly regulated by kinases, via both the KCNQ1  $\alpha$  subunit, and the KCNE1  $\beta$  subunit as we show here.

## Conclusions and clinical implications

The current findings elucidate the long sought-after mechanism by which PKC reduces  $I_{Ks}$  density: stimulation of KCNE1-mediated, clathrin- and dynamin-dependent, endocytosis of the KCNQ1-KCNE1 potassium channel complex. The unique aspect of this type of  $\beta$  subunit-mediated internalization is that it can, as we demonstrate herein and previously,<sup>16</sup> regulate not just current density but also gating kinetics because it favors a relative increase in KCNQ1 complexes lacking KCNE1. The discovery that PKC downregulation of  $I_{Ks}$  requires dynamin, and presumably adaptor proteins involved in clathrin-mediated endocytosis, may lead to searches for small molecules to disrupt or facilitate interaction of KCNE1 with these proteins, as an alternative therapeutic avenue to control  $I_{Ks}$  density and gating kinetics. Because PKC is activated by  $\alpha$ 1 adrenergic stimulation, such therapeutics could be used to blunt the changes observed in  $I_{Ks}$  upon abrupt autonomic activation, which are potentially life threatening in individuals with loss-of-function KCNQ1 mutations.

## Acknowledgments

The authors thank Dr. Geri Kreitzer and Dr. Roberto Levi (Weill Cornell Medical College) for invaluable feedback during this study.

## References

1. Deusch C. Potassium channel ontogeny. *Annu Rev Physiol* 2002;64:19–46.
2. McCrossan ZA, Abbott GW. The MinK-related peptides. *Neuropharmacology* 2004;47:787–821.
3. Barhanin J, Lesage F, Guillemare E, et al. K(V)LQT1 and IsK (minK) proteins associate to form the I(Ks) cardiac potassium current. *Nature* 1996;384:78–80.
4. Freeman LC, Kass RS. Expression of a minimal K<sup>+</sup> channel protein in mammalian cells and immunolocalization in guinea pig heart. *Circ Res* 1993;73:968–973.
5. Sesti F, Goldstein SA. Single-channel characteristics of wild-type IKs channels and channels formed with two minK mutants that cause long QT syndrome. *J Gen Physiol* 1998;112:651–663.
6. Sanguinetti MC, Curran ME, Zou A, et al. Coassembly of K(V)LQT1 and minK (IsK) proteins to form cardiac I(Ks) potassium channel. *Nature* 1996;384:80–83.
7. Marcus DC, Shen Z. Slowly activating voltage-dependent K<sup>+</sup> conductance is apical pathway for K<sup>+</sup> secretion in vestibular dark cells. *Am J Physiol* 1994; 267:C857–864.
8. Vetter DE, Mann JR, Wangemann P, et al. Inner ear defects induced by null mutation of the isk gene. *Neuron* 1996;17:1251–1264.
9. Pusch M, Magrassi R, Wollnik B, Conti F. Activation and inactivation of homomeric KvLQT1 potassium channels. *Biophys J* 1998;75:785–792.
10. Seeböhm G, Sanguinetti MC, Pusch M. Tight coupling of rubidium conductance and inactivation in human KCNQ1 potassium channels. *J Physiol* 2003;552: 369–378.
11. Tyson J, Tranebjaerg L, Bellman S, et al. IsK and KvLQT1: mutation in either of the two subunits of the slow component of the delayed rectifier potassium channel can cause Jervell and Lange-Nielsen syndrome. *Hum Mol Genet* 1997; 6:2179–2185.
12. Splawski I, Tristani-Firouzi M, Lehmann MH, Sanguinetti MC, Keating MT. Mutations in the hminK gene cause long QT syndrome and suppress IKs function. *Nat Genet* 1997;17:338–340.
13. Neyroud N, Tesson F, Denjoy I, et al. A novel mutation in the potassium channel gene KVLQT1 causes the Jervell and Lange-Nielsen cardioauditory syndrome. *Nat Genet* 1997;15:186–189.
14. Herbert E, Trusz-Gluzka M, Moric E, et al. KCNQ1 gene mutations and the respective genotype-phenotype correlations in the long QT syndrome. *Med Sci Monit* 2002;8:RA240–248.
15. Choi G, Kopplin LJ, Tester DJ, et al. Spectrum and frequency of cardiac channel defects in swimming-triggered arrhythmia syndromes. *Circulation* 2004;110: 2119–2124.
16. Xu X, Kanda VA, Choi E, et al. MinK-dependent internalization of the IKs potassium channel. *Cardiovasc Res* 2009;82:430–438.
17. Varnum MD, Busch AE, Bond CT, Maylie J, Adelman JP. The min K channel underlies the cardiac potassium current IKs and mediates species-specific responses to protein kinase C. *Proc Natl Acad Sci U S A* 1993;90:11528–11532.
18. Zhang ZJ, Jurkiewicz NK, Folander K, et al. K<sup>+</sup> currents expressed from the guinea pig cardiac IsK protein are enhanced by activators of protein kinase C. *Proc Natl Acad Sci U S A* 1994;91:1766–1770.
19. Honore E, Attali B, Romey G, et al. Cloning, expression, pharmacology and regulation of a delayed rectifier K<sup>+</sup> channel in mouse heart. *Embo J* 1991;10: 2805–2811.
20. Henrich CJ, Simpson PC. Differential acute and chronic response of protein kinase C in cultured neonatal rat heart myocytes to alpha 1-adrenergic and phorbol ester stimulation. *J Mol Cell Cardiol* 1988;20:1081–1085.
21. Homma N, Hirasawa A, Shibata K, Hashimoto K, Tsujimoto G. Both alpha(1A)- and alpha(1B)-adrenergic receptor subtypes couple to the transient outward current (I(To)) in rat ventricular myocytes. *Br J Pharmacol* 2000;129:1113–1120.
22. Lewis A, McCrossan ZA, Abbott GW. MinK, MiRP1, and MiRP2 diversify Kv3.1 and Kv3.2 potassium channel gating. *J Biol Chem* 2004;279:7884–7892.
23. Li Q, Lau A, Morris TJ, et al. A syntaxin 1, Galpha(o), and N-type calcium channel complex at a presynaptic nerve terminal: analysis by quantitative immunocolocalization. *J Neurosci* 2004;24:4070–4081.
24. Diatloff-Zito C, Gordon AJ, Duchaud E, Merlin G. Isolation of an ubiquitously expressed cDNA encoding human dynamin II, a member of the large GTP-binding protein family. *Gene* 1995;163:301–306.
25. Zhang J, Barak LS, Winkler KE, Caron MG, Ferguson SS. A central role for beta-arrestins and clathrin-coated vesicle-mediated endocytosis in beta2-adrenergic receptor resensitization. Differential regulation of receptor resensitization in two distinct cell types. *J Biol Chem* 1997;272:27005–27014.
26. Pearse BM. Coated vesicles from human placenta carry ferritin, transferrin, and immunoglobulin G. *Proc Natl Acad Sci U S A* 1982;79:451–455.
27. Nuss HB, Marban E. Electrophysiological properties of neonatal mouse cardiac myocytes in primary culture. *J Physiol* 1994;479:265–279.
28. Wang L, Feng ZP, Kondo CS, Sheldon RS, Duff HJ. Developmental changes in the delayed rectifier K<sup>+</sup> channels in mouse heart. *Circ Res* 1996;79:79–85.
29. Reinhardt J, Kosch M, Lerner M, et al. Stimulation of protein kinase C pathway mediates endocytosis of human nongastric H<sup>+</sup>-K<sup>+</sup>-ATPase, ATP1A1. *Am J Physiol Renal Physiol* 2002;283:F335–343.
30. Seeböhm G, Strutz-Seeböhm N, Birkin R, et al. Regulation of endocytic recycling of KCNQ1/KCNE1 potassium channels. *Circ Res* 2007;100:686–692.
31. Jespersen T, Membrez M, Nicolas CS, et al. The KCNQ1 potassium channel is down-regulated by ubiquitylating enzymes of the Nedd4/Nedd4-like family. *Cardiovascular Research* 2007;74:64–74.
32. Alesutan I, Foller M, Sopjani M, et al. Inhibition of the heterotetrameric K<sup>+</sup> channel KCNQ1/KCNE1 by the AMP-activated protein kinase. *Mol Membr Biol* 2011;28:79–89.
33. Marx SO, Kurokawa J, Reiken S, et al. Requirement of a macromolecular signaling complex for beta adrenergic receptor modulation of the KCNQ1-KCNE1 potassium channel. *Science* 2002;295:496–499.
34. Grimmer S, van Deurs B, Sandvig K. Membrane ruffling and macropinocytosis in A431 cells require cholesterol. *J Cell Sci* 2002;115:2953–2962.